RSC Advances

PAPER

View Article Online
View Journal | View Issue

Cite this: *RSC Adv.*, 2023, **13**, 23130

The volatile release evaluation of nicotine from snus products under different storage conditions based on surface-enhanced Raman spectroscopy technology†

Yongfeng Tian,[ab] Lu Zhao,[c] Yonghua Pan,[d] Zhengfeng Li,[e] Xiaofeng Shen,[a] Xia Zhang,[a] Xianghu Tang, *[bf] Xin Feng*[a] and Xingjiu Huang [bf]

Surface enhanced Raman spectroscopy (SERS) is a highly sensitive analytical detection technique that provides unique chemical and structural information on target molecules. Snus is a type of tobacco product that can release nicotine and other components under certain humidity and temperature without burning, and the evaluation of its nicotine release under different storage conditions is very important for understanding its characteristics, regulating its components, and setting reasonable storage conditions. Herein, by means of an artificial climate box and suction extraction device, the volatile release evaluations of nicotine from snus products under different storage conditions were performed based on Fe_3O_4 microparticles coated with Au nanorods and Au nanoparticles (Fe_3O_4@AuNRsNPs) as SERS substrates combined with a capillary. The Fe_3O_4@AuNRsNPs assemblies can be fixed in the inner wall of the capillary with the aid of an external magnetic field, which improved the maneuverability of the SERS substrates. By comparing the intensities of the spectral peaks of the symmetrical breathing of the pyridine moiety of nicotine molecules with increasing temperature and humidity, which could significantly accelerate the volatile release of a small amount of nicotine, the nicotine release under different conditions could be evaluated. Based on this strategy, it was possible to obtain the storage or placement conditions of the product. The results of this study provide a reference to clarify the volatile release of nicotine under various storage conditions, which is helpful for better regulation of the levels of nicotine in snus. Moreover, such destruction-free evaluation of the volatile release of nicotine from snus products under different storage conditions opens up new perspectives for further research about the impact of nicotinoids on smokers' health and cessation programs.

Received 14th June 2023
Accepted 14th July 2023

DOI: 10.1039/d3ra03977c

rsc.li/rsc-advances

Introduction

Nowadays, it is generally accepted that smoking, including passive smoking caused by smoke, is harmful to health.[1–3] However, it is still difficult for the masses of smokers who use tobacco to ameliorate anxiety and mental health problems to keep away from tobacco products.[4–6] Smokeless tobacco is considered less harmful than smoking, *e.g.*, it does not cause passive smoking, which makes many smokers who have trouble quitting switch to smokeless products,[7–9] such as snus,[10–12] which contain leaf tobacco or non-tobacco plant materials infused with nicotine, and are used by placing pouches in the mouth, allowing the nicotine to be absorbed through the lining of the mouth at a continuous rate until it is removed. Despite reducing the risks of passive smoking, a plethora of snus products lead to unacceptable exposure to multiple potentially harmful substances, which is a possible cause of oral diseases. Moreover, unlike traditional tobacco, snus products can release nicotine at lower temperatures without burning. Because of these, some viewpoints propose that the regulation of the levels of toxicants and nicotine in snus products and evidence-based tobacco control efforts have been recognized as established pathways to prevent tobacco related diseases.[13] Therefore, in order to understand the impact of nicotinoids on smokers' health and cessation programs, and to clarify the nicotine

[a]*Technology Center of China Tobacco Yunnan Industrial Co., Ltd., Kunming 650231, China. E-mail: fengx@ynzy-tobacco.com*

[b]*Key Laboratory of Environmental Optics and Technology, Anhui Institute of Optics and Fine Mechanics, HFIPS, Chinese Academy of Sciences, Hefei 230031, China. E-mail: tangxh2011@iim.ac.cn*

[c]*Yunnan Academy of Tobacco Agricultural Sciences, Kunming 650000, China*

[d]*Hongta Tobacco (Group) Co., Ltd., Yuxi 653100, China*

[e]*The Raw Material Center of China Tobacco Yunnan Industrial Co., Ltd., Kunming 650231, China*

[f]*Institute of Solid State Physics, HFIPS, Chinese Academy of Sciences, Hefei 230031, China*

† Electronic supplementary information (ESI) available. See DOI: https://doi.org/10.1039/d3ra03977c

volatile release under various storage conditions, as well as to achieve better regulation of the levels of toxicants and nicotine in snus, it is necessary to conduct relevant studies to rapidly and reliably evaluate the release of nicotine from snus products.

However, due to the slow and extremely small amount volatilization of nicotine from snus under normal conditions, it is difficult to achieve the evaluation of its volatilization by conventional methods. Therefore, no other rapid detection methods have been reported to evaluate the volatilization of nicotine from snus yet. But, among the various analytical detection methods, surface enhanced Raman spectroscopy (SERS) is a highly sensitive analytical method and rapid confirmatory detection technique that provides unique chemical and structural information on target molecules and has achieved widespread application in the qualitative analysis of substances,[14–17] and is expected to be used for the volatile release evaluations of nicotine from snus products under different storage conditions. Here, it is worth mentioning that the development and application of SERS technology depend on the design of the substrates as well as the construction of the corresponding module.[17–22] For many more substrates, especially practical SERS substrates, their current development needs to consider the characteristics of high reliability, fast operation, easy maintenance and portability.[23–25] Researchers found that binary nano- or micro-particles composed of a superparamagnetic core and Au or Ag nanoshell, such as Fe_3O_4 microparticles coated with Au nanorods (Fe_3O_4@AuNRs),[26] Fe_3O_4 coated with Au nanoparticles (Fe_3O_4@AuNPs),[27] *etc.*, have a lot of advantages.[27–29] These nanoscale noble metal nanoshell-coated magnetic particles would be useful, especially in the SERS analysis of chemical species dissolved in aqueous solutions because the magnetic particles can be readily enriched from the solution by means of an external magnetic field without centrifugation or filtration. Meanwhile, the binary SERS substrate combined with a capillary structure,[30–32] which is semi-closed, can be used as an embedded SERS substrate or for building micro circulation research.[33–35] Besides, according to our previous research,[36] as one type of highly volatile analyte, conducting nicotine's identification based on SERS in a relatively closed or semi-closed state should be better. Meanwhile, in view of the fact that the regulated growth optimization of construction of a type of AuNP assembly hierarchical structure in the capillary (AuNPs/Cap)[36] is still a complicated process, nanoscale noble metal nanoshell-coated magnetic particles combined with a capillary to construct a microflow path module provide a potential optimization research strategy with more maneuverability for release evaluation of nicotine from snus products.

Herein, based on the above considerations, in this study, we put forward the research idea of the volatile release evaluation of nicotine from snus products under different storage conditions based on SERS technology by means of Fe_3O_4 microparticles coated with AuNRs and AuNPs (Fe_3O_4@AuNRsNPs) combined with a capillary. The co-assembly of AuNRs and AuNPs on the surface of Fe_3O_4 has a higher SERS sensitivity. Through the investigation of volatile release of nicotine, the nicotine release or migration rate of snus products under certain conditions can be used for establishing a method for rapid evaluation of the storage or placement conditions of the products. In addition, such destruction-free simultaneous extraction and SERS detection of nicotine in snus products open up new perspectives for better regulation of the levels of nicotine in snus, as well as for further research about the impact of nicotinoids on smokers' health and cessation programs.

Experimental

Materials

L-Ascorbic acid (AA, 99%), tetrachloroauric acid tetrahydrate ($HAuCl_4 \cdot 4H_2O$), cetyltrimethylammonium bromide (CTAB, 99%), silver nitrite ($AgNO_3$), nitric acid (HNO_3), polyethylene glycol (PEG), iron(III) chloride hexahydrate ($FeCl_3 \cdot 6H_2O$), ethylene glycol (EG), sodium acetate anhydrous ($NaAc \cdot 3H_2O$), trisodium citrate ($C_6H_5Na_3O_7$), sodium borohydride ($NaBH_4$), poly(vinylpyrrolidone) (PVP, k30) and polyethylenimine (PEI) were purchased from Shanghai Chemical Reagent Company (Shanghai, China). The reagents were all of analytical grade and used without further purification. Ultrapure water (>18.0 MΩ·cm) was purified using a Millipore Milli-Q gradient system throughout the experiment.

Synthesis of Fe_3O_4 microspheres

The synthesis of Fe_3O_4 was carried out according to the literature.[26,37] Typically, first, 2.7 g $FeCl_3 \cdot 6H_2O$ was dissolved in 80 mL EG. Then, 2.0 g PEG (molecular weight 10 000) and 7.2 g $NaAc \cdot 3H_2O$ were added to the solution. The mixture was stirred until the reactants were fully dissolved. And then, the mixture was transferred into a Teflon®-lined autoclave with a capacity of 100 mL and heated at 200 °C for 12 h. After the product was rinsed alternately with ethanol and pure water several times with the aid of an external magnetic field, it was dried under vacuum at 60 °C for 6 h.

Synthesis of AuNPs and AuNRs

AuNPs were synthesized by reduction of $HAuCl_4$ with trisodium citrate.[38] Briefly, 2 mL (1% wt) $C_6H_5Na_3O_7$ solution was quickly added to a boiling $HAuCl_4$ solution (100 mL, 0.25 mM) under reflux and vigorous stirring. After boiling for 40 min, the heating mantle was removed to let the solution cool to room temperature for further use.

AuNRs were synthesized using the seed growth method.[39] Briefly, Au seeds were initially synthesized by carrying out a $NaBH_4$ reduction of $HAuCl_4$, and then AuNRs were obtained by seed growth regulation. After that, the solution of these AuNRs was transferred into centrifuge tubes, and the product was collected by centrifugation at 7.5 rpm and washed with pure water twice in order to remove the excess CTAB. And then, AuNRs were transferred into 5 mg mL^{-1} PVP ethanol solution for surface functionalization with PVP.[40] After the PVP was allowed to adsorb onto the surface of Au NRs for 12 h with stirring, the solution was centrifuged at 7.5 rpm to remove excess PVP, and then it was redispersed in ethanol before use.

Fabrication of AuNR and AuNP coated Fe_3O_4 microparticles

First, 50 mg Fe_3O_4 microparticles were functionalized with PEI by suspending them in 25 mL 5 mg mL^{-1} PEI solution. After washing with pure water several times, the PEI-functionalized Fe_3O_4 microparticles were dispersed into PVP-stabilized AuNR solution, followed by shaking for about 4 h in an incubator shaker. After that, the products were redispersed in 10 mL water with ultrasonication within minutes. And then, Fe_3O_4@AuNRs particles were functionalized with PEI by suspending them in 25 mL 5 mg mL^{-1} PEI solution. After washing with pure water several times, the PEI-treated Fe_3O_4@AuNRs particles were dispersed into AuNP solution. The reaction was allowed to proceed at room temperature for 4 h under continuous shaking in an incubator shaker. The resulting products were collected by a magnet, followed by washing with water. After that, the products Fe_3O_4@AuNRsNPs were redispersed in 10 mL water with ultrasonication prior to further use.

Volatile release evaluation of nicotine from snus products under different storage conditions based on SERS

Scheme 1 displays the schematic illustration of the volatile release evaluation of nicotine from snus products under different storage conditions based on SERS. By setting the temperature, humidity and other conditions of the artificial climate storage chamber, the snus pouch was put into the storage chamber for a certain period of time, respectively, and then transferred into the air extraction chamber. The volatile components on the surface of the snus products will follow the air flow, and the water-soluble molecules such as nicotine would remain in the water filter module (similar to a water pipe). After the micro pump worked for 10 min, the SERS detection module was connected, and the liquid in the water filter entered into the capillary, which was loaded with Fe_3O_4@AuNRsNPs microparticles. After staying for 5 min, SERS detection was carried out, and the Raman spectrum collection time was about 5 s.

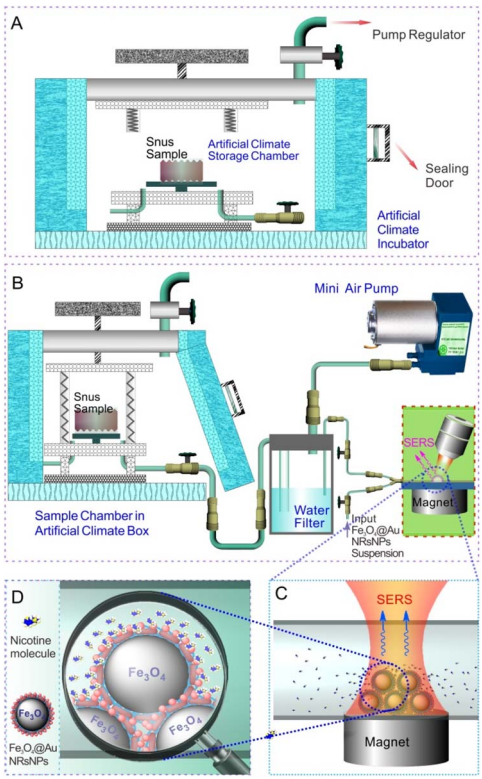

Scheme 1 (A) Schematic illustration of different storage conditions based on an artificial climate storage chamber. (B) Schematic illustration of the volatile release evaluation of nicotine from snus products under different storage conditions based on Fe_3O_4@AuNRsNPs combined with a capillary to construct a SERS detection module. (C) and (D) Schematic illustrations of the Fe_3O_4@AuNRsNPs substrate combined with a capillary for SERS detection of nicotine from snus and Fe_3O_4@AuNRsNPs microparticle assemblies.

Characterization and instruments

The morphology, structure, and composition of the samples were investigated by using an Auriga focused ion-beam scanning electron microscope (FIB-SEM), and a JEOL JEM-2010 high-resolution transmission electron microscope (HRTEM) equipped with an Oxford INCA energy dispersive spectroscopy (EDS) system, respectively. The absorption spectra were obtained using a UV-2550 spectrophotometer. Raman spectra were recorded on a LabRAM HR800 confocal microscope Raman system (Horiba Jobin Yvon). The laser beam was focused on the sample using a 10× LMPLFLN microscope objective (numerical aperture NA = 0.25; working distance WD = 10.6 mm). The Raman spectrometer was calibrated using a silicon wafer at 520.7 cm^{-1}. The laser power was approximately 1 mW. For each SERS spectrum, baseline correction was performed using LabSpec V5.58.25 software, and the peak frequency was obtained from peak fitting.

Results and discussion

Fig. 1A displays a schematic illustration of the principle procedure for the fabrication of AuNR and AuNP coated Fe_3O_4 microparticles. The surfaces of citrate-AuNPs and PVP functionalized AuNRs[40] employed in this work were negatively charged, while the surfaces of PEI functionalized Fe_3O_4 or Fe_3O_4@AuNRs microparticles were positively charged due to a large number of basic amino groups at the polymer chains of PEI,[26] thus making the assembly of AuNPs and AuNRs on the surfaces of microspheres based on the electrostatic interaction. The formation of AuNRs, Au NPs, Fe_3O_4 and Fe_3O_4@AuNRs microparticles was characterized by SEM, TEM, and UV-vis absorption spectra, respectively (Fig. S1 and S2, ESI†). Typical digital photos of Fe_3O_4 and Fe_3O_4@AuNRs-NPs dispersion liquid and the corresponding assembly with the aid of an external magnetic field can be seen in Fig. 1B and C, respectively. As can be seen from the figure, both Fe_3O_4 and Fe_3O_4@AuNRsNPs exhibit superparamagnetism under the action of an external magnetic field. The evidence for the co-assembly of AuNRs and AuNPs on the surface of Fe_3O_4 was confirmed by SEM, TEM and EDS, as shown in Fig. 1D–H. Fig. 1D and E show the typical SEM images of Fe_3O_4@AuNRs-NPs microparticles at

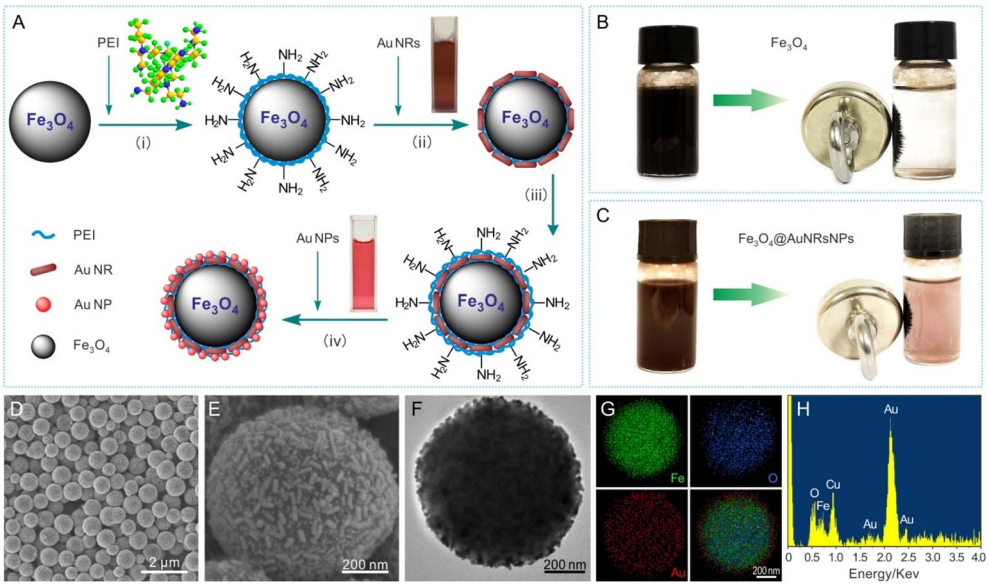

Fig. 1 (A) Schematic illustration of the procedure for the fabrication of AuNR and AuNP coated Fe_3O_4 microspheres. (B) and (C) Typical digital photos of Fe_3O_4 and Fe_3O_4@AuNRsNPs dispersion liquid and the corresponding assembly with the aid of an external magnetic field, respectively. (D) and (E) Typical SEM images of Fe_3O_4@AuNRsNPs microparticles at different magnifications. (F) Typical TEM image of a single particle of Fe_3O_4@AuNRsNPs. (G) EDS of Fe_3O_4@AuNRsNPs microparticles and elemental mappings of Fe, O, and Au corresponding to (F). (H) EDS spectrum of Fe_3O_4@AuNRsNPs microparticles corresponding to (G).

different magnifications. It is clear that the sample was composed of many dispersed Fe_3O_4@AuNRsNPs microparticles with diameters of 500–800 nm. Moreover, as can be clearly seen from Fig. 1F, the TEM image also indicated that the Fe_3O_4 microparticles were coated with AuNRs and AuNPs. This is because, as previously mentioned, AuNRs employed in this work were pretreated with PVP and the surface was negatively charged, and the surface of the citrate stabilized AuNPs was negatively charged, while the surfaces of PEI-functionalized Fe_3O_4 microspheres were positively charged[26] due to a large number of basic amino groups at the polymer chains of PEI, thus making the assembly of AuNRs and AuNPs on the surfaces of Fe_3O_4 microspheres based on the electrostatic interaction. In order to further investigate the elemental distribution of the Fe_3O_4@AuNRsNPs, the elemental mappings of Fe, O, and Au were also performed by EDS area scans corresponding to Fig. 1F, as shown in Fig. 1G. Meanwhile, EDS spectrum analysis can be seen in Fig. 1H. Fig. 1G and H indicate that the as-prepared product consists of Fe, O, and Au. As a note, the Cu element was detected in the sample, originating from copper grids. From Fig. 1G, the profile of Au element is similar to but slightly larger than those of O and Fe, which indicates that the Au element distributes densely and surrounds the Fe_3O_4 microparticle core. It is worth mentioning that there were many gaps of several manometers between Au nanostructures, which would be very advantageous for forming hot spots, and achieving large near-field enhancement effects, and beneficial for SERS activity.

To evaluate the potential application of the as-obtained Fe_3O_4@AuNRsNPs microparticles combined with a capillary to construct a SERS detection module, nicotine standard solution was chosen as the probe molecule. Fig. 2A and B show the typical digital photos of SERS detection of nicotine based on Fe_3O_4@AuNRsNPs combined with a capillary to construct a SERS detection module and Fe_3O_4@AuNRsNPs microparticles assembled with the aid of an external magnetic field. With the entry of the liquid containing probe molecules, when a certain concentration of nicotine molecules approached and stayed on the surface of Fe_3O_4@AuNRsNPs in the inner wall of the

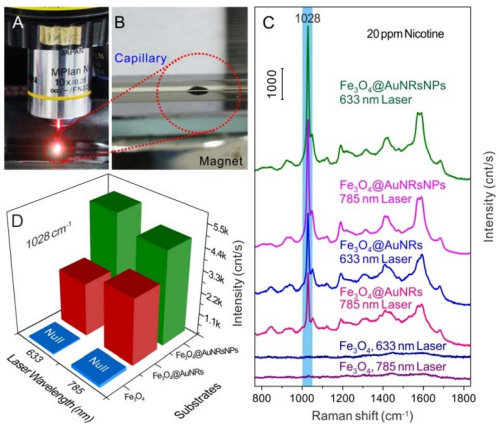

Fig. 2 (A) Typical digital photo of SERS detection based on Fe_3O_4@AuNRsNPs combined with a capillary to construct a SERS detection module. (B) Fe_3O_4@AuNRsNPs microparticles assembled with the aid of an external magnetic field. (C) A series of SERS spectra of nicotine in water at 20 ppm with different assembled structures as SERS substrates in the capillary, respectively. (D) Comparison of the intensities of the peak position at 1028 cm^{-1} of 20 ppm nicotine based on different assembled structure SERS substrates corresponding to (C).

capillary, its SERS signal may be detected under laser excitation. Fig. 2C shows the series of SERS spectra of nicotine in water at 20 ppm with different assembled structures as SERS substrates in the capillary, respectively. As shown in Fig. 2C, it can be found that either Fe_3O_4@AuNRsNPs or Fe_3O_4@AuNRs was used as the SERS substrate, and 20 ppm of nicotine exhibited a dominant peak at 1028 cm^{-1}, a shoulder at 1049 cm^{-1}, and other smaller peaks. Compared with the normal Raman spectrum of nicotine from our previous research[36] and ref. 41–43, the peaks at 1028 cm^{-1} and 1049 cm^{-1} are tentatively assigned to the symmetrical breathing and trigonal ring deformation of the pyridine moiety. Meanwhile, when only Fe_3O_4 microspheres were used as the substrates, the results showed that almost no nicotine-related Raman signals were detected, which also indicates that the AuNRs or AuNRsNPs accumulated on the surface of Fe_3O_4 microparticles had Raman enhancement effect. By comparing the peak intensities at 1028 cm^{-1} of different SERS substrates, as can be seen in Fig. 2C and D, it can be further found that Fe_3O_4@AuNRsNPs showed a more significant effect than Fe_3O_4@AuNRs, regardless of whether the laser wavelength was 633 nm or 785 nm. The reason for this result involves the structure of the AuNRs or AuNRsNPs assemblies. It is generally believed that plasma resonance effect with high density "hot spots" between nanostructures is the key aspect to the SERS effect.[44–46] By co-assembling AuNPs on the surface of Fe_3O_4@AuNRs, Raman enhancement effect was significantly improved compared with the initial assembled structure due to the optimization of density and particle gap and other structures. Therefore, the optimal substrate, Fe_3O_4@AuNRsNPs, was used in the subsequent study.

Fig. 3A shows the SERS spectra of different concentrations of nicotine with Fe_3O_4@AuNRsNPs as substrates combined with a capillary and water as the dispersion medium. When low concentration of nicotine adsorbed on or approached the surface of Au nanostructures, a SERS signal would be detected. From the result, it can be found that standard nicotine solution can be detected as low as 0.2 ppm, which proved the sensitivity of the SERS technology with Fe_3O_4@AuNRsNPs as SERS substrates for nicotine identification. In order to evaluate the practical application significance of Fe_3O_4@AuNRsNPs as SERS substrates combined with a capillary, 20 ppm nicotine solution flowed into the capillary, and SERS detection was carried out after ~5 min. Because of the unique structural of capillary, its capillary action will be available for the liquid directly be absorbed, without any auxiliary tools. And the capillary structure is a semi-closed state, so it is not easily contaminated followed by the construction of micro circulation, which can be used for a new type of SERS detection module and can keep the nicotine molecules from escaping by volatilization under the monitoring process, as shown in Fig. 3B and C. Although the SERS signals based on Fe_3O_4@AuNRsNPs combined with the capillary also fluctuated to a certain extent, the amplitude of fluctuation was less than 15%, and the signal intensities remained relatively stable. In addition, the Raman peak at 1028 cm^{-1} was chosen to calculate the relative standard deviation (RSD) of different spectra to evaluate the reproducibility of Fe_3O_4@AuNRsNPs. The value of RSD in different batches from Fe_3O_4@AuNRsNPs is 11.97% (more details can be seen in Fig. S3, ESI†), presenting an acceptable variation (less than 20% RSD) in SERS intensities.[47] Therefore, through combining the advantages such as SERS effect, reproducibility and maneuverability of the substrates, Fe_3O_4@AuNRsNPs microparticles combined with a capillary are suitable for the detection and monitoring of nicotine and other highly volatile analytes.

Snus is a type of tobacco product that can release nicotine and other components under certain humidity and temperature without burning, and the evaluation of its nicotine release under different storage conditions is very important for understanding its characteristics, regulating its components and setting reasonable storage conditions. Thus, the volatile release evaluation of nicotine from snus products under different storage conditions based on SERS technology by means of Fe_3O_4@AuNRsNPs microparticles combined with a capillary was carried out according to Scheme 1 (more details can be seen in Fig. S4, ESI†). By setting the temperature, humidity and other conditions of the artificial climate storage chamber, the snus pouch (typical snus powder and snus pouch can be seen in Fig. 4A and B) was put into the storage chamber for a certain period of time, typically, 24 h, 48 h and 72 h, respectively, and then transferred into the air extraction chamber. Some of the volatile components on the surface of the snus will follow the air flow, and the water-soluble molecules such as nicotine would mainly remain in the water filter module, which can be seen in Fig. 4C. After the micro pump worked for 10 min, the SERS detection module was connected, and the liquid in the water filter entered into the capillary loaded with Fe_3O_4@AuNRsNPs. After staying for 5 min, SERS detection was carried out. It's worth noting that the Fe_3O_4@AuNRsNPs assemblies were fixed in the inner wall of the capillary with the aid of an external magnetic field, which also improved the maneuverability of the SERS substrates. As can be seen from Fig. 4D–F, increasing temperature could significantly accelerate the release of a small amount of volatiles of nicotine.

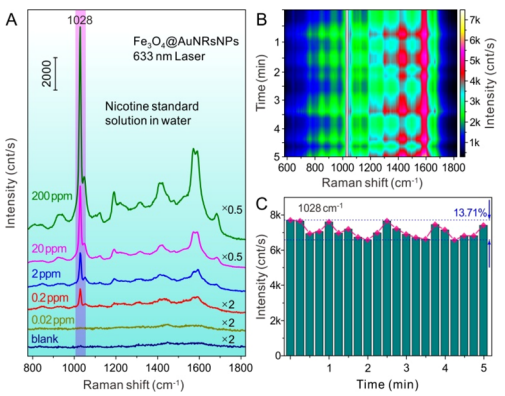

Fig. 3 (A) A series of SERS spectra of nicotine in water at different concentrations with Fe_3O_4@AuNRsNPs as the SERS substrates combined with a capillary, respectively. (B) Time-dependent SERS spectra of 20 ppm nicotine based on Fe_3O_4@AuNRsNPs combined with a capillary. (C) Time-dependent SERS intensity fluctuation of nicotine based on Fe_3O_4@AuNRsNPs substrates combined with a capillary.

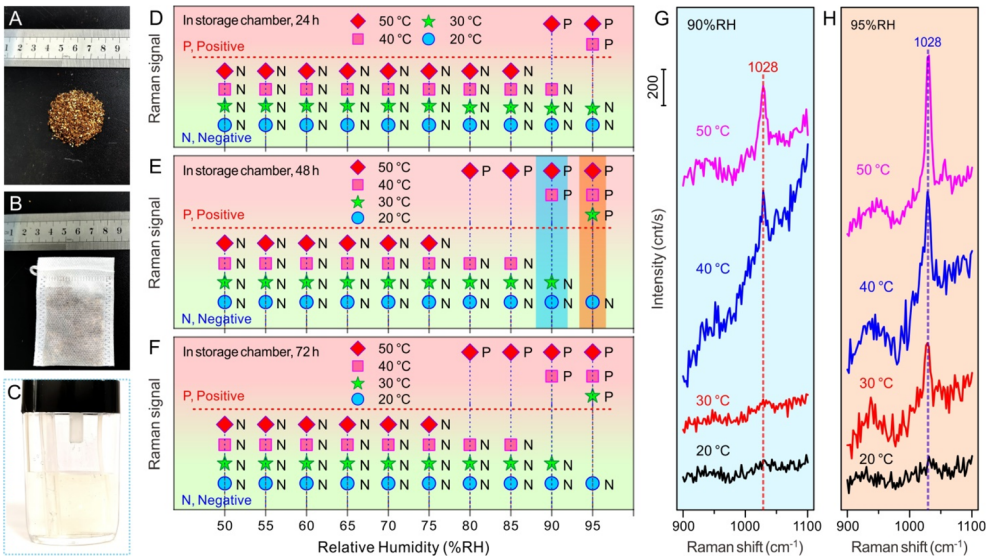

Fig. 4 Typical digital photos of (A) snus powder and (B) snus pouch. (C) Typical digital photos of the water filter module. (D)–(F) By means of an artificial climate box and suction extraction device, the volatile release evaluations of nicotine from snus products under different storage conditions were carried out based on SERS technology. Typical release evaluations of nicotine from the snus pouch based on Fe_3O_4@AuNRsNPs SERS substrates combined with a capillary under different conditions for SERS detection: placed in the storage chamber for 48 hours (G) at 90% RH and (H) at 95% RH.

From Fig. 4, it can be further seen that when the temperature increased under high humidity, the volatiles of nicotine were released more significantly. For example, when the temperature increased to 30 °C under 95% RH, the SERS signal of nicotine could be detected after 10 min of pumping with a micro-pump, and while the temperature increased to 50 °C under 95% RH, the SERS signal became superconspicuous. Through the comparative study between Fig. 4G and H, we can also find that, when stored at the same temperature and with higher humidity, volatile nicotine is released much more easily. Taking 30 °C storage as an example, when the humidity was 95% RH, the SERS signal of nicotine could be detected after 10 min of pumping using a micro-pump; on the contrary, at 90% RH, the relevant Raman signal is almost undetectable. Furthermore, from Fig. 4D–F, it can also be found that, at low temperature and low humidity, the length of storage time has little effect on the volatile release of nicotine from the snus pouch. And at higher temperatures, *e.g.*, more than 30 °C, and higher humidity, *e.g.*, more than 80% RH, the volatile release of nicotine from snus shows a trend from slow to fast, and then to smooth release. By comparing Fig. 4F and E, we can see that there is almost no change between the two. Based on the above results, it can be found that, in order to reduce the potential harm caused by the volatile release of nicotine from snus in the process of storage and transportation, in addition to packaging and other factors, it is necessary to reduce the humidity of the surroundings, such as less than 80% RH, and lower the temperature, such as lower than 30 °C. Moreover, the results of this study provide a reference to clarify the nicotine volatile release under various storage conditions, which is helpful for better regulation of the levels of nicotine in snus.

Conclusions

In summary, by means of an artificial climate box and suction extraction device, the volatile release evaluations of nicotine from snus products under different storage conditions were performed based on Fe_3O_4@AuNRsNPs SERS substrates combined with a capillary. The Fe_3O_4@AuNRsNPs assemblies can be fixed in the inner wall of the capillary with the aid of an external magnetic field, which improved the maneuverability of the SERS substrates. And compared to Fe_3O_4@AuNRs, Fe_3O_4@AuNRsNPs showed a more significant SERS effect, regardless of whether the laser excitation wavelength was 633 nm or 785 nm. Besides, based on this strategy, it was possible to obtain the storage or placement conditions of the snus products. Through comparison of the intensities of the spectral peaks of the symmetrical breathing of pyridine moiety of nicotine molecules, increasing temperature and higher humidity could significantly accelerate the release of a small amount of volatiles of nicotine. Thus, in order to reduce the potential harm caused by the volatile release of nicotine from snus in the process of storage and transportation, it is necessary to reduce the humidity of the surroundings, *e.g.*, less than 80% RH, and lower the temperature, *e.g.*, lower than 30 °C. The results of this study provide a reference to clarify the nicotine volatile release under various storage conditions, which is helpful for better regulation of the levels of nicotine in snus. Moreover, such destruction-free evaluation of volatile release of nicotine from snus products under different storage conditions opens up new perspectives for further research about the impact of nicotinoids on smokers' health and cessation programs.

Conflicts of interest

There are no conflicts of interest to declare.

Acknowledgements

We thank Prof. Donglai Zhu and Prof. Yunhua Qin for discussions.

Notes and references

1 J. Kim, H. Song, J. Lee, Y. J. Kim, H. S. Chung, J. M. Yu, G. Jang, R. Park, W. Chung, C.-M. Oh and S. Moon, *Sci. Rep.*, 2023, **13**, 3878.
2 Y. L. Zhang, J. F. Liu, L. Zhang, L. Jin, N. D. E. Greene, Z. W. Li and A. G. Ren, *China CDC Wkly.*, 2021, **3**, 778–782.
3 T. K. Burki, *Lancet Oncol.*, 2021, **22**, 1217.
4 U. Daood, M. N. Bijle, S. S. Mahdi, H. Omar and S. Bilal, *Vib. Spectrosc.*, 2021, **114**, 103235.
5 Y. Li, A. E. Burns, L. N. Tran, K. A. Abellar, M. Poindexter, X. Li, A. K. Madl, K. E. Pinkerton and T. B. Nguyen, *Chem. Res. Toxicol.*, 2021, **34**, 1640–1654.
6 M. Fluharty, A. E. Taylor, M. Grabski and M. R. Munafò, *Nicotine Tob. Res.*, 2016, **19**, 3–13.
7 S. B. Shaikh, C. Newton, W. C. Tung, Y. Sun, D. Li, D. Ossip and I. Rahman, *Int. J. Environ. Res. Public Health*, 2023, **20**, 4526.
8 L. S. Bast, M. B. Klitgaard, S. G. Kjeld, N. S. Jarlstrup and A. I. Christensen, *Int. J. Environ. Res. Public Health*, 2022, **19**, 5623.
9 K. A. East, J. L. Reid, V. L. Rynard and D. Hammond, *J. Adolesc. Health*, 2021, **69**, 447–456.
10 T. Tjora, J. C. Skogen and B. Sivertsen, *Nicotine Tob. Res.*, 2022, **25**, 135–142.
11 E. Clarke, K. Thompson, S. Weaver, J. Thompson and G. O'Connell, *Harm Reduct. J.*, 2019, **16**, 62.
12 L. E. Rutqvist, M. Curvall, T. Hassler, T. Ringberger and I. Wahlberg, *Harm Reduct. J.*, 2011, **8**, 11.
13 S. S. Hecht and D. K. Hatsukami, *Nat. Rev. Cancer*, 2022, **22**, 143–155.
14 Y. Zhou, Y. Lu, Y. Liu, X. Hu and H. Chen, *Biosens. Bioelectron.*, 2023, **228**, 115231.
15 T. Itoh, M. Procházka, Z. Dong, W. Ji, Y. S. Yamamoto, Y. Zhang and Y. Ozaki, *Chem. Rev.*, 2023, **123**, 1552–1634.
16 S. L. Kitaw, Y. S. Birhan and H.-C. Tsai, *Environ. Res.*, 2023, **221**, 115247.
17 H. Liu, K. Zhan, K. Wang and X. Xia, *TrAC, Trends Anal. Chem.*, 2023, **159**, 116939.
18 N. R. Visaveliya, R. Mazetyte Stasinskiene and J. M. Köhler, *Adv. Opt. Mater.*, 2022, **10**, 2102757.
19 O. Guselnikova, H. Lim, H. J. Kim, S. H. Kim, A. Gorbunova, M. Eguchi, P. Postnikov, T. Nakanishi, T. Asahi, J. Na and Y. Yamauchi, *Small*, 2022, **18**, 2107182.
20 D. Lin, T. Qin, Y. Wang, X. Sun and L. Chen, *ACS Appl. Mater. Interfaces*, 2014, **6**, 1320–1329.
21 M. Kasztelan, A. Studzinska, G. Z. Żukowska and B. Pałys, *Front. Chem.*, 2021, **9**, 665205.
22 D. Gao, X. Yang, M. Luo, P. Teng, H. Zhang, Z. Liu, S. Gao, Z. Li, X. Wen, L. Yuan, K. Li, M. Bowkett and N. Copner, *ACS Appl. Nano Mater.*, 2021, **4**, 10784–10790.
23 X. Fu, Y. Wang, Y. Liu, H. Liu, L. Fu, J. Wen, J. Li, P. Wei and L. Chen, *Analyst*, 2019, **144**, 1582–1589.
24 J. He, X. Li and J. Li, *J. Environ. Chem. Eng.*, 2022, **10**, 108278.
25 Y.-B. Kwon, S. Y. Cho, H. Jang, J.-H. Kim and Y.-K. Kim, *Langmuir*, 2021, **37**, 14205–14213.
26 X. Tang, R. Dong, L. Yang and J. Liu, *J. Raman Spectrosc.*, 2015, **46**, 470–475.
27 T. Xie, D. Xu, Y. Shang, Y. Li, Y. Gu, G. Yang and L. Qu, *Sens. Actuators, B*, 2023, **375**, 132897.
28 Y. Li, W. Duan and J. Wei, *ACS Appl. Nano Mater.*, 2021, **4**, 4181–4188.
29 L. B. Berganza, L. Litti, M. Meneghetti, S. Lanceros-Méndez and J. Reguera, *ACS Omega*, 2022, **7**, 45493–45503.
30 Z. Huang, S. Siddhanta, G. Zheng, T. Kickler and I. Barman, *Angew. Chem., Int. Ed.*, 2020, **59**, 5972–5978.
31 M. Zhang, J. Pan, X. Xu, G. Fu, L. Zhang, P. Sun, X. Yan, F. Liu, C. Wang, X. Liu and G. Lu, *Anal. Chem.*, 2022, **94**, 4850–4858.
32 Q. Ma, K. Minoshima and S. Shoji, *J. Phys. Chem. A*, 2023, **127**, 378–383.
33 Y. Yu, P. Zeng, C. Yang, J. Gong, R. Liang, Q. Ou and S. Zhang, *ACS Appl. Nano Mater.*, 2019, **2**, 598–606.
34 S. Lin, W. Hasi, X. Lin, S. Han, T. Xiang, S. Liang and L. Wang, *ACS Sens.*, 2020, **5**, 1465–1473.
35 Y. Han, X. Fang, Z. Sun, C. Kang, L. Zha and X. Zhang, *ACS Appl. Nano Mater.*, 2022, **5**, 2445–2450.
36 Y. Tian, X. Tang, Y. Fu, S. Shang, G. Dong, T. Li, X. Huang and D. Zhu, *Anal. Methods*, 2021, **13**, 5608–5616.
37 Z. Liu, Y. Wang, R. Deng, L. Yang, S. Yu, S. Xu and W. Xu, *ACS Appl. Mater. Interfaces*, 2016, **8**, 14160–14168.
38 X. Tang, W. Cai, L. Yang and J. Liu, *Nanoscale*, 2013, **5**, 11193–11199.
39 X. Ye, L. Jin, H. Caglayan, J. Chen, G. Xing, C. Zheng, V. Doan-Nguyen, Y. Kang, N. Engheta, C. R. Kagan and C. B. Murray, *ACS Nano*, 2012, **6**, 2804–2817.
40 M. Mao, B. Zhou, X. Tang, C. Chen, M. Ge, P. Li, X. Huang, L. Yang and J. Liu, *Chem.–Eur. J.*, 2018, **24**, 4094–4102.
41 J. Y. Chien, Y. C. Gu, H. M. Tsai, C. H. Liu, C. Y. Yen, Y. L. Wang, J. Wang and C. H. Lin, *J. Food Drug Anal.*, 2020, **28**, 108–114.
42 B. Lin, J. Chen, Y. Zeng, L. Li, B. Qiu, Z. Lin and L. Guo, *ACS Sens.*, 2019, **4**, 1844–1850.
43 N. Itoh and S. E. J. Bell, *Analyst*, 2017, **142**, 994–998.
44 M. Ge, P. Li, G. Zhou, S. Chen, W. Han, F. Qin, Y. Nie, Y. Wang, M. Qin, G. Huang, S. Li, Y. Wang, L. Yang and Z. Tian, *J. Am. Chem. Soc.*, 2021, **143**, 7769–7776.
45 X. Wang, C. Liu, C. Gao, K. Yao, S. S. M. Masouleh, R. Berté, H. Ren, L. d. S. Menezes, E. Cortés, I. C. Bicket, H. Wang, N. Li, Z. Zhang, M. Li, W. Xie, Y. Yu, Y. Fang, S. Zhang, H. Xu, A. Vomiero, Y. Liu, G. A. Botton, S. A. Maier and H. Liang, *ACS Nano*, 2021, **15**, 10553–10564.
46 A. I. Pérez-Jiménez, D. Lyu, Z. Lu, G. Liu and B. Ren, *Chem. Sci.*, 2020, **11**, 4563–4577.

47 J. Langer, D. Jimenez de Aberasturi, J. Aizpurua, R. A. Alvarez-Puebla, B. Auguié, J. J. Baumberg, G. C. Bazan, S. E. J. Bell, A. Boisen, A. G. Brolo, J. Choo, D. Cialla-May, V. Deckert, L. Fabris, K. Faulds, F. J. García de Abajo, R. Goodacre, D. Graham, A. J. Haes, C. L. Haynes, C. Huck, T. Itoh, M. Käll, J. Kneipp, N. A. Kotov, H. Kuang, E. C. Le Ru, H. K. Lee, J.-F. Li, X. Y. Ling, S. A. Maier, T. Mayerhöfer, M. Moskovits, K. Murakoshi, J.-M. Nam, S. Nie, Y. Ozaki, I. Pastoriza-Santos, J. Perez-Juste, J. Popp, A. Pucci, S. Reich, B. Ren, G. C. Schatz, T. Shegai, S. Schlücker, L.-L. Tay, K. G. Thomas, Z.-Q. Tian, R. P. Van Duyne, T. Vo-Dinh, Y. Wang, K. A. Willets, C. Xu, H. Xu, Y. Xu, Y. S. Yamamoto, B. Zhao and L. M. Liz-Marzán, *ACS Nano*, 2020, **14**, 28–117.